

末次冰盛期以来中国东南沿海地区的气候变化特征及驱动机制

王晨艺^{1,2,3}

¹福建师范大学地理研究所, 福建 福州

²福建师范大学地理科学学院, 福建 福州

³福建师范大学湿润亚热带生态-地理过程教育部重点实验室, 福建 福州

收稿日期: 2026年1月3日; 录用日期: 2026年2月20日; 发布日期: 2026年3月4日

摘要

末次冰盛期作为地球气候系统演化的关键转折点, 对中国东南沿海地区的气候格局与生态演变具有重要影响。然而, 现有研究在定量解析海洋因素作用、高分辨率气候重建及多驱动机制耦合研究等方面仍存在显著不足。因此, 本研究聚焦于中国东南沿海地区, 系统整合了包括孢粉、湖泊/泥炭沉积物等18条地质记录, 运用Z-scores标准化分析与局部加权回归平滑处理(LOESS), 重建了末次冰盛期以来中国东南沿海地区的气候演变过程, 并深入探讨了其驱动机制。主要得出以下结论: (1) 末次冰盛期以来, 中国东南沿海地区气候变化显著, 经历了多次冷暖、干湿交替阶段, 可划分为以下三个阶段: ① 25,000~15,000 yr B.P. (末次冰盛期), 中国东南沿海地区以冷干气候为主, 且在千年尺度上存在显著振荡; ② 15,000~10,000 yr B.P. (末次冰消期), 中国东南沿海地区可能存在两种不同的气候模式; ③ 10,000 yr B.P. (全新世以来), 中国东南沿海地区的气候变化存在不稳定性, 不同区域间的气候特征存在显著差异。(2) 全新世以来, 太阳辐射是驱动中国东南沿海地区气候变化的主要外部因素, 太阳辐射通过影响亚洲夏季风的强度, 主导区域气候周期性变化。此外, 热带海气环流传输和放大了太阳活动的影响, 赤道辐合带(ITCZ)的南北移动及厄尔尼诺-南方涛动(ENSO)活动是中国东南沿海地区气候变化的重要因素。本研究通过多源数据耦合与定量分析, 完善了末次冰盛期以来中国东南沿海地区气候变化及驱动机制等研究方面的不足, 为理解中国东南沿海地区气候系统演变机制及预测未来气候变化提供了关键科学依据。

关键词

末次冰盛期, 中国东南沿海, 定量重建, 气候变化, 驱动机制

Climate Change Characteristics and Driving Mechanisms in Southeast Coastal China since the Last Glacial Maximum

Chenyi Wang^{1,2,3}

¹Institute of Geography, Fujian Normal University, Fuzhou Fujian

²School of Geographical Sciences, Fujian Normal University, Fuzhou Fujian

³Key Laboratory for Humid Subtropical Eco-Geographical Processes of the Ministry of Education, Fujian Normal University, Fuzhou Fujian

Received: January 3, 2026; accepted: February 20, 2026; published: March 4, 2026

Abstract

The Last Glacial Maximum (LGM), as a pivotal turning point in the evolution of the Earth's climate system, has exerted a profound impact on the climate pattern and ecological evolution in the southeast coastal region of China. However, existing research still exhibits significant deficiencies in quantitatively analyzing the role of marine factors, conducting high-resolution climate reconstruction, and studying the coupling of multiple driving mechanisms. Therefore, this study focuses on the southeast coastal region of China. It systematically integrates 18 geological records, including pollen and lake/peat sediments. By employing Z-scores standardization analysis and Locally Weighted Regression Smoothing (LOESS), we have reconstructed the climate evolution process in the southeast coastal region of China since the LGM and delved deeply into its driving mechanisms. The main conclusions are as follows: (1) Since the LGM, the climate in the southeast coastal region of China has undergone remarkable changes, experiencing multiple alternating phases of cold-warm and dry-wet conditions, which can be divided into the following three stages: ① From 25,000 to 15,000 yr B.P. (during the LGM), the southeast coastal region of China was predominantly characterized by a cold and dry climate, with significant oscillations on a millennial scale; ② From 15,000 to 10,000 yr B.P. (during the last deglaciation), two distinct climate patterns may have existed in the southeast coastal region of China; ③ Since 10,000 yr B.P. (since the Holocene), the climate change in the southeast coastal region of China has been unstable, with significant differences in climate characteristics among different regions. (2) Since the Holocene, solar radiation has been the primary external factor driving climate change in the southeast coastal region of China. Solar radiation influences the intensity of the Asian summer monsoon, thereby dominating the periodic changes in regional climate. Additionally, tropical ocean-atmosphere circulation transmits and amplifies the impact of solar activity. The north-south movement of the Intertropical Convergence Zone (ITCZ) and El Niño-Southern Oscillation (ENSO) activities are important factors influencing climate change in the southeast coastal region of China. Through multi-source data coupling and quantitative analysis, this study has addressed the research gaps in climate change and driving mechanisms in the southeast coastal region of China since the LGM, providing crucial scientific evidence for understanding the evolution mechanism of the climate system and predicting future climate change in this region.

Keywords

Last Glacial Maximum, Southeast Coastal China, Quantitative Reconstruction, Climate Change, Driving Mechanism

Copyright © 2026 by author(s) and Hans Publishers Inc.

This work is licensed under the Creative Commons Attribution International License (CC BY 4.0).

<http://creativecommons.org/licenses/by/4.0/>



Open Access

1. 引言

末次冰盛期(Last Glacial Maximum, LGM), 作为距今最近的一个与现代气候环境反差最大的时期, 是指北半球辐射降低、海表温度减小、CO₂ 和 CH₄ 浓度降低和大陆冰盖(冰川)达到最大的时期[1]。尽管世

界各地冰量达到最大的时间不完全一致[2]，但多数地区约为 26.5~19 ka [3]。此时段全球平均海平面下降 120~140 m [4] [5]，海水盐度增大。南北中高纬地区增大的冰盖促使南北两极地区温度下降，北半球植被带向北退缩，沙漠面积扩大和黄土积淀迅速[6]。这些变化引起了全球海-气重组，导致全球水汽循环发生显著变化。末次冰盛期、末次冰消期和全新世是 3 个连续且具有截然不同冰量边界条件的典型气候期。其中，冰盛期和全新世具有完全不同的地球轨道背景，是整个地质历史气候期中气候背景差异最大的两个时期，研究末次冰盛期以来的气候变化有助于揭示地球气候系统在自然驱动因素作用下的长期演变规律，为理解气候系统的复杂机制提供关键证据。

中国东南沿海地区，作为连接陆地与海洋的关键过渡带，其气候变化不仅受全球冰期-间冰期旋回的调控，还受到东亚季风系统、海平面波动及地形地貌的复杂影响[7]。通过重建末次冰盛期以来中国东南沿海地区的气候变化序列，分析其与东亚季风系统等驱动因素之间的关系，揭示东亚季风区在不同气候背景下的响应模式和驱动机制，为完善全球气候变化理论提供重要依据。同时，有助于深入研究气候系统各要素之间的相互作用和反馈机制，提高对气候系统复杂性的认识和理解[7]。

目前，国内外研究学者已对末次冰盛期以来的全球气候变化进行了相关研究，对末次冰盛期以来全球气候系统的基本特征和变化规律得出相关结论[1]-[7]。但现有研究多聚焦于内陆黄土高原或青藏高原地区的单一区域或单一指标研究，针对中国东南沿海地区的系统研究相对薄弱[8] [9]。此外，对东南沿海地区末次冰盛期以来的气候重建多依赖间接证据，缺乏数据之间的整合分析以及对气候变化区域响应机制的研究[10]。鉴于现有研究存在的局限性，本研究通过整合中国东南沿海地区 18 条古气候记录，通过 Z-scores 分析等方法，系统性地重建了中国东南沿海地区末次冰盛期以来的气候变化。本研究主要解决以下问题：(1) 中国东南沿海地区末次冰盛期以来的气候变化特征；(2) 全新世以来中国东南沿海气候气候变化的驱动机制。

2. 研究区域

中国东南沿海地区(20°~28°N, 110°~125°E)，东接太平洋、南邻南海、西倚武夷山脉-南岭山脉、北界与长江三角洲气候过渡区(以 7 月 300 mm 等降水量线为标准)相接。地形以低海拔平原与丘陵为主。气候受东亚夏季风雨带季节性移动主导，是雨带初始登陆并早期停留的核心区域，呈现双峰型降水模式：5~6 月梅雨锋降水形成主峰，受中纬度西风带与季风气流耦合控制，降水持续时间长、范围广；8~9 月热带气旋活动引发次峰，降水强度大、局地性强，台风降水贡献率达年总量 35%~50%。该区域年降水量自沿海向内陆递减，但降水日数递增，暴雨频次占全国 25%，兼具季风区与热带气候过度特征，夏季风爆发初期呈“干湿交替”现象，是研究季风降水极端化与气候过渡性的关键区域[11] [12]。

3. 数据来源与方法

3.1. 气候记录的选择

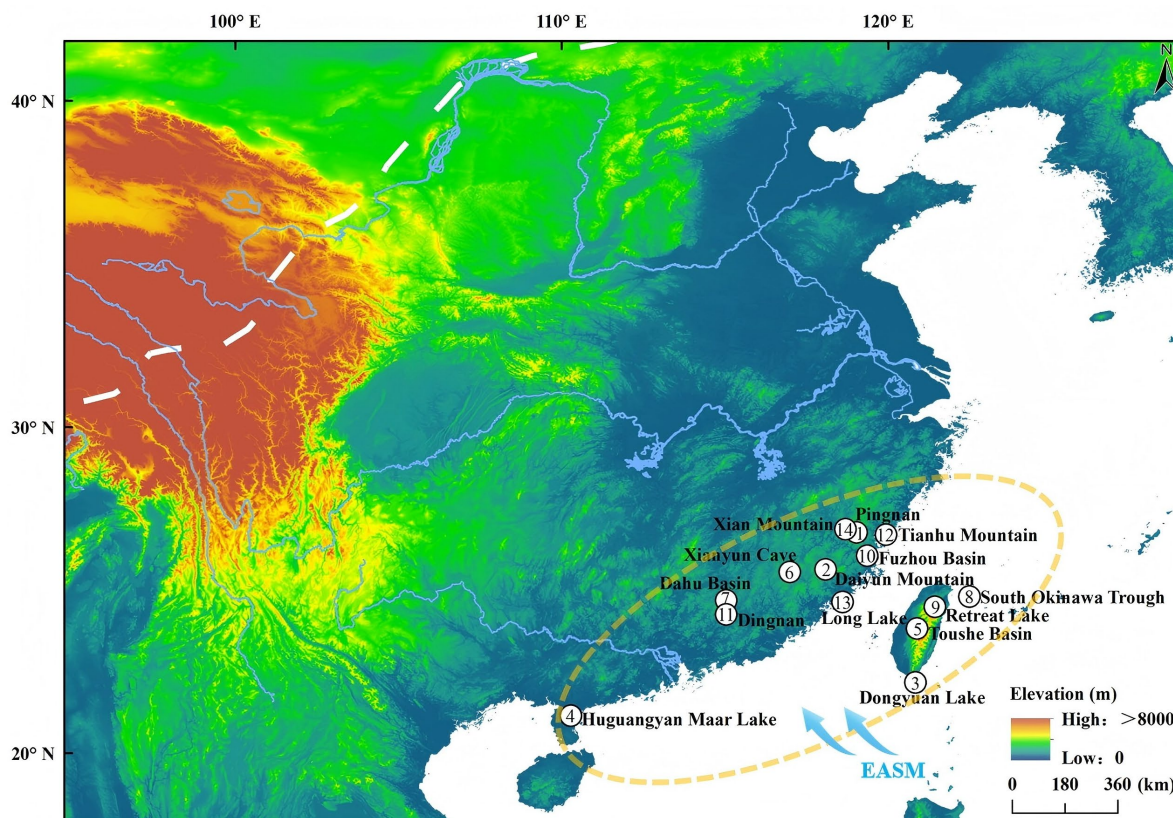
本研究共收集了中国东南沿海地区的 18 条地质记录(图 1)(表 1)。地质记录载体包括湖泊岩芯、河流/泥炭沉积剖面、石笋等。地质记录选择的标准为：具备完整的年代框架、测年序列完整、年代误差可控，且代用指标具有一定的指示意义并达到足够的分辨率。此外，18 条地质记录与气候之间存在相关性，记录的变化能够反映气候冷暖、干湿条件的变化。

3.2. 代用指标的指示意义

反映气候水热条件变化的指标包括地球物理数据、地球化学数据及生物数据(表 1)。

地球物理磁学方法通过识别磁性矿物的占比、粒度特征等来重建过去的气候变化。洱海沉积物的磁

化率(MS)可反映不同水热条件下由湖泊侵蚀所带来的淤泥/细砂含量,及其中所含原生磁铁矿的含量[13]。此外,在黄土高原地区,磁化率还可以反映受降水控制的成土过程,作为风尘沉积物水分变化的代用指标[14]。



注: 该图基于自然资源部标准底图服务网站下载的审图号: GS(2016)1590 号的标准地图制作, 底图无修改。黄色虚线圆圈代表本研究所界定的中国东南沿海地区的区域范围。蓝色箭头代表东亚夏季风。白色虚线代表中国季风区与非季风区分界线[13]。

Figure 1. The geographical location map of the selected geological record

图 1. 所选地质记录所在的地理位置图

地球化学方法有助于研究环境与气候变化之间的关系。沉积物中的有机质(TOM、TOC、TON、C/N等)可以直接反映有机输入量、古生产力及沉积后的气候条件。在湖泊和沼泽系统中,存在两大主要生产来源:原生水生植物(生长于湖泊水体)和外来陆地植物(生长于湖泊流域),两者对水体生物群落、流域植被及湖泊生产力产生影响。C/N 比值可以指示区域植被类型和生物量,进而反映区域降水变化。TOM、TOC 与 TON 比值的升高指示温暖湿润气候条件下的降水增加;相反,比值的降低指示寒冷干燥气候条件下的降水减少[15]-[17]。有机质含量(Organic content)和腐殖化程度(Humification degree)对气候环境变化响应敏感,同样可以反映区域气候波动[15]-[17]。此外,稳定同位素指标也可以指示气候变化,陆源有机质 $\delta^{13}\text{C}_{\text{org}}$ 值的变化可作为 C3 和 C4 植被类型变化的代用指标[18],进而反映区域气候条件变化;高分辨率石笋 $\delta^{18}\text{O}$ 用于指示局地湿度变化与水汽来源或季风强度之间的关系[19] [20]。

生物方法中的孢粉作为植被演替的直接标志,其形态学特征可鉴定至科水平,进而量化重建水热交替驱动的植被类型转变[21] [22]。在季风影响区,降水增加通过 C3 木本植被扩张和 C4 草本植被限制,形成孢粉组合中木本和草本植被比例的正相关波动;基于数据分析方法,可将植被类型变化转换为降水

定量值，反映区域干湿变化[21] [22]。

3.3. 方法

为提高时间序列数据的信噪比并量化异常波动，本研究对所选取的 18 条数据记录进行了分析处理。

3.3.1. 数据平滑处理

采用局部加权回归(LOESS, Locally Estimated Scatterplot Smoothing)对原始数据进行平滑，以消除短期噪声干扰。平滑窗口宽度设定为总数据长度的 20% (即 3 个数据点)，权重函数选用三次多项式，通过迭代优化(迭代次数 = 5)使均方根误差(RMSE)最小化。数据平滑处理使原始数据在保留长期趋势的同时，有效抑制了高频波动[23]。

3.3.2. Z-Scores 标准化分析

由于 18 条记录包含不同量纲的指标，需统一至无量纲标准正态分布(均值 = 0，标准差 = 1)，以实现跨指标异常值识别与气候信号耦合分析[24]。

对平滑后的数据序列进行标准化处理，计算每个数据点的 Z-score 值：

$$Z_i = \frac{X_i - \mu}{\sigma} \quad (1)$$

其中 X_i 为第 i 个数据点， μ 和 σ 分别为序列的均值与标准差。通过 Z-scores 标准化分析将数据序列转换为均值为 0、标准差为 1 的标准化变量，使不同量纲的记录具备可比性[24]。以均值 0 为标准，大于 0/小于 0 来反映区域气候条件的变化。

Table 1. Detailed information of the climate records referred to in the text with key references. See Figure 1 for location
表 1. 文中提及的气候记录详细信息及关键参考文献。地理位置见图 1

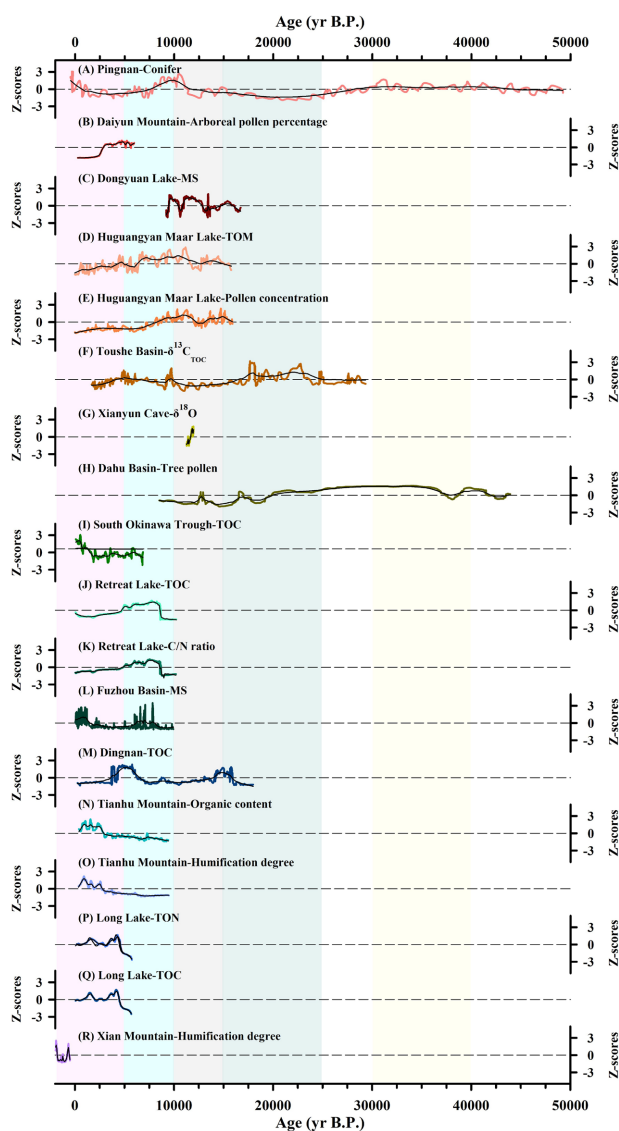
Site No.	Site	Lat. (N°)	Long. (E°)	Archive	Proxies	Reference
1	Pingnan	26.46	119.02	Lake core	Pollen	Yue <i>et al.</i> , 2012
2	Daiyun Mountain	25.38	118.05	Peat section	Pollen	Zhao <i>et al.</i> , 2017
3	Dongyuan Lake	22.10	120.50	Lake core	MS	Ding <i>et al.</i> , 2016
4	Huguangyan Maar Lake	21.90	110.17	Lake core	TOM; Pollen	Wang <i>et al.</i> , 2016
5	Toushe Basin	23.49	120.53	Lake core	$\delta^{13}\text{C}_{\text{TOC}}$	Li <i>et al.</i> , 2013
6	Xianyun Cave	25.33	116.59	Stalagmite	$\delta^{18}\text{O}$	Cui <i>et al.</i> , 2018
7	Dahu Basin	24.41	115.02	Lake core	Pollen	Chen <i>et al.</i> , 2019
8	South Okinawa Trough	24.48	122.29	Lake core	TOC	Chen <i>et al.</i> , 2018
9	Retreat Lake	24.29	121.26	Lake core	TOC; C/N ratio	Selvaraj <i>et al.</i> , 2011
10	Fuzhou Basin	26.03	119.21	Lake core	MS	Yue <i>et al.</i> , 2015
11	Dingnan	24.15	115.20	Lake core	TOC	Zhou <i>et al.</i> , 2005
12	Tianhu Mountain	26.42	119.56	Peat section	Organic content; Humification degree	Zhang <i>et al.</i> , 2012
13	Long Lake	24.38	118.36	Lake core	TON; TOC	Wang <i>et al.</i> , 2009
14	Xian Mountain	26.52	118.41	Peat section	Humification degree	Hu <i>et al.</i> , 2012

MS: Magnetic susceptibility; TOM: Total Organic Matter; TOC: Total Organic Carbon; TON: Total Organic Nitrogen.

4. 结果

4.1. 植被与孢粉指标

福建屏南孢粉记录显示, 50,000 yr B.P.以来, 其 Z-score 值在早期至中期相对稳定, 晚期出现波动, 表明该区域植被组成在千年尺度上具有一定稳定性, 但也存在阶段性变化(图 2(A)) [25]。福建戴云山山地高山孢粉记录的 Z-score 值在全新世晚期呈下降趋势, 指示区域植被从以高山植被为主向其他类型植被的转变过程(图 2(B)) [26]。大湖盆地树木孢粉的 Z-score 值在 40,000~20,000 yr B.P.期间相对平稳, 在 20,000~10,000 yr B.P.期间小于均值, 表明该区域森林植被在 40,000~20,000 yr B.P.期间相对稳定, 20,000~10,000 yr B.P.期间有缩减趋势(图 2(H)) [27]。



淡黄色、淡绿色、淡红色、淡蓝色、淡粉色条带分别代表 40,000~30,000 yr B.P.、25,000~15,000 yr B.P.、15,000~10,000 yr B.P.、10,000~5,000 yr B.P.及 5,000 yr B.P.以来的 5 个时段。黑色实线代表各个记录指标经过平滑处理后的曲线。黑色虚线代表各个记录指标的平均值。18 条记录指标均通过 Z-scores 标准化分析。

Figure 2. Comparison of paleoclimate records in the southeastern coastal region of China since the Last Glacial Maximum
图 2. 末次冰盛期以来中国东南沿海地区的古气候记录对比

4.2. 湖泊/泥炭沉积指标

Dongyuan 湖沉积物的磁化率在 20,000~10,000 yr B.P 期间波动显著,反映了湖泊沉积环境的复杂性,包括有机质来源、沉积速率等多种因素的综合作用(图 2(C)) [28]。广东湖光岩玛珉湖沉积物的总有机质(图 2(D)) [29]和孢粉浓度(图 2(E)) [29]的 Z-score 值变化表明,该湖泊在 15,000 yr B.P.以来经历了多次有机质输入和孢粉沉积的变化,与区域气候的干湿交替密切相关。Retreat 湖沉积物 C/N 比的 Z-score 值变化反映了有机质来源,高 C/N 比指示陆源有机质输入增加,反映区域暖湿的气候条件(图 2(K)) [30]。

Toushe 盆地沉积物的 $\delta^{13}\text{C}_{\text{TOC}}$ 变化反映了植被类型(C3/C4 植被)以及碳循环过程的改变(图 2(F)) [31]。南海冲绳海槽沉积物的总有机碳(图 2(I)) [32], Retreat 湖沉积物的总有机碳(图 2(J)) [30]以及定南沉积物总有机碳(图 2(M)) [33]的 Z-score 值变化反映了不同区域有机碳含量的变化,进而反映区域气候条件变化。

福建福州盆地沉积物的磁化率(图 2(L)) [34]和福建天湖山沉积物有机质含量(图 2(N)) [35]的 Z-score 值变化反映了不同沉积环境的差异以及有机质的积累过程。福建天湖山沉积物的腐殖化程度(图 2(O)) [35],福建龙湖沉积物总有机氮(图 2(P)) [36]、总有机碳(图 2(Q)) [36]及福建仙山沉积物腐殖化程度(图 2(R)) [37]的 Z-score 值变化反映了不同区域土壤或沉积物中有机质的分解和积累状态,指示区域气候环境条件的变化。

5. 讨论

5.1. 40,000 yr B.P.以来,中国东南沿海地区气候变化特征

5.1.1. 40,000~30,000 yr B.P. (末次冰盛期早期寒冷阶段)

40,000~30,000 yr B.P.期间,福建屏南(图 2(A)) [25]及大湖盆地(图 2(H)) [28]孢粉记录的 z-score 值波动较小,表明在该时段内,研究区域内的气温、降水等气候要素未出现剧烈波动,植被类型未发生显著变化,整体气候格局较为稳定。

5.1.2. 25,000~15,000 yr B.P. (末次冰盛期)

福建屏南孢粉记录的 Z-score 值小于均值,指示该区域在末次冰盛期以冷干气候条件为主(图 2(A)) [25]。Dongyuan 湖沉积物磁化率记录的 Z-score 值在 17,500~15,000 yr B.P.期间虽存在波动,但整体变化小于均值,表明该区域以冷干的气候特征为主(图 2(C)) [28]。Toushe 盆地沉积物的 $\delta^{13}\text{C}_{\text{TOC}}$ 在 25,000~15,000 yr B.P.期间偏正,其 Z-score 值大于均值,表明区域内 C3 木本植被的减少和 C4 草本植被的增加,指示区域冷干气候条件(图 2(F)) [31]。大湖盆地树木孢粉记录的 Z-score 值在末次冰盛期期间以 20,000 yr B.P.为分界点存在波动,25,000~20,000 yr B.P.的 Z-score 值大于均值,表明区域暖湿气候条件;20,000~15,000 yr B.P.的 Z-score 值显著下降,降至均值以下,表明区域冷干气候条件,指示该区域在千年尺度上存在气候振荡现象(图 2(H)) [28]。定南沉积物总有机碳的 Z-score 值在 17,500~15,000 yr B.P.期间也存在显著波动,指示区域气候条件从暖湿转变为冷干(图 2(M)) [34]。

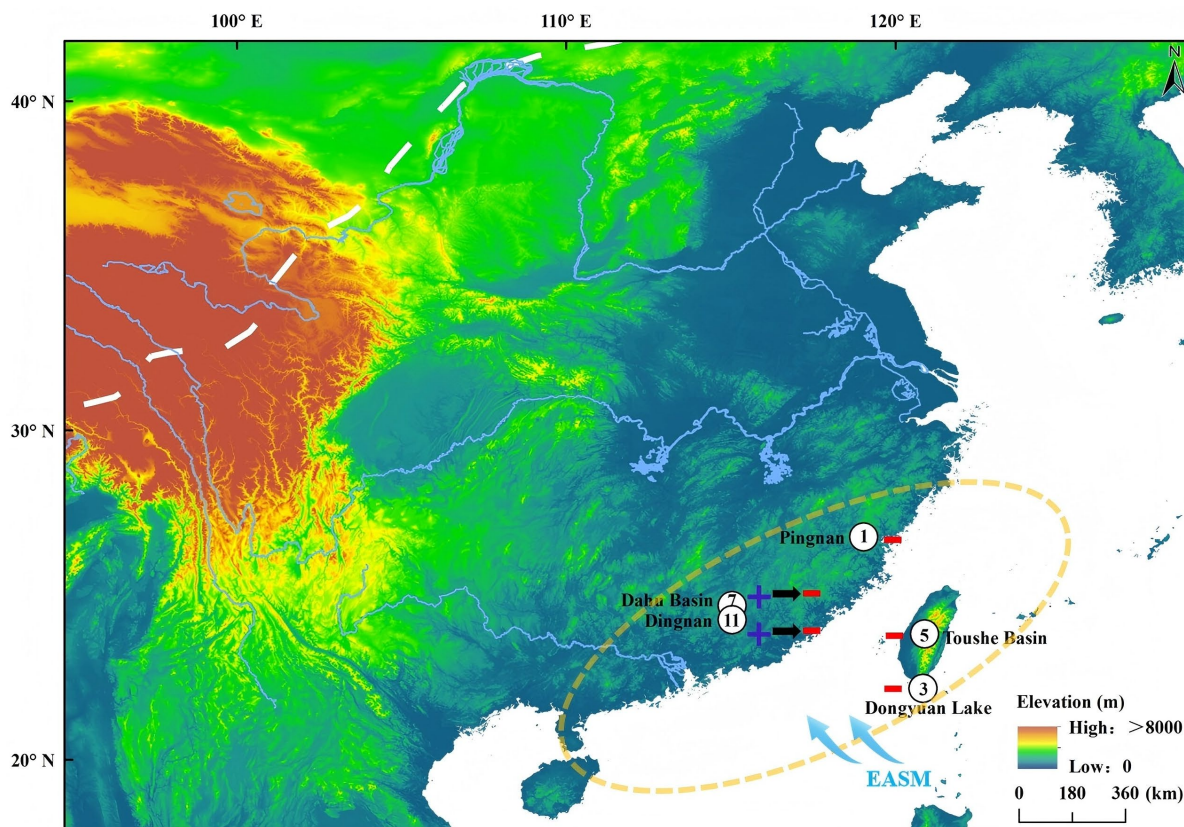
综上,末次冰盛期期间,中国东南沿海地区以冷干气候条件为主,在千年尺度上存在气候振荡(图 2)(图 3)。

5.1.3. 15,000~10,000 yr B.P. (末次冰消期)

福建屏南孢粉记录(图 2(A)) [25],福建仙云洞石笋记录(图 2(G)) [38],大湖盆地树木孢粉记录(图 2(H)) [28]及定南沉积物总有机碳记录(图 2(M)) [34] Z-score 值均小于均值,指示区域以冷干的气候条件为主。相反, Dongyuan 湖沉积物磁化率(图 2(C)) [28],广东湖光岩玛珉湖沉积物总有机质(图 2(D)) [29]、孢粉浓度(图 2(E)) [29]记录的 Z-score 值均大于均值,指示区域气候条件的暖湿。此外, Toushe 盆地沉积物

$\delta^{13}\text{C}_{\text{TOC}}$ 记录在 15,000~10,000 yr B.P. 期间偏负, 其 Z-score 值小于均值, 表明区域内 C3 木本植物的增加, 指示区域暖湿气候条件(图 2(F)) [31]。

综上, 末次冰消期期间, 中国东南沿海地区可能存在两种不同的气候模式(图 2) (图 4)。



注: 该图基于自然资源部标准地图服务网站下载的审图号: GS(2016)1590 号的标准地图制作, 底图无修改。黄色虚线圆圈代表本研究所界定的中国东南沿海地区的区域范围。蓝色箭头代表东亚夏季风。白色虚线代表中国季风区与非季风区分界线[13]。加号代表区域暖湿的气候特征, 减号代表区域冷干的气候特征。黑色箭头代表区域气候条件的转变过程。

Figure 3. Climatic characteristics of the southeastern coastal region of China during the Last Glacial Maximum

图 3. 末次冰盛期中国东南沿海地区的气候特征

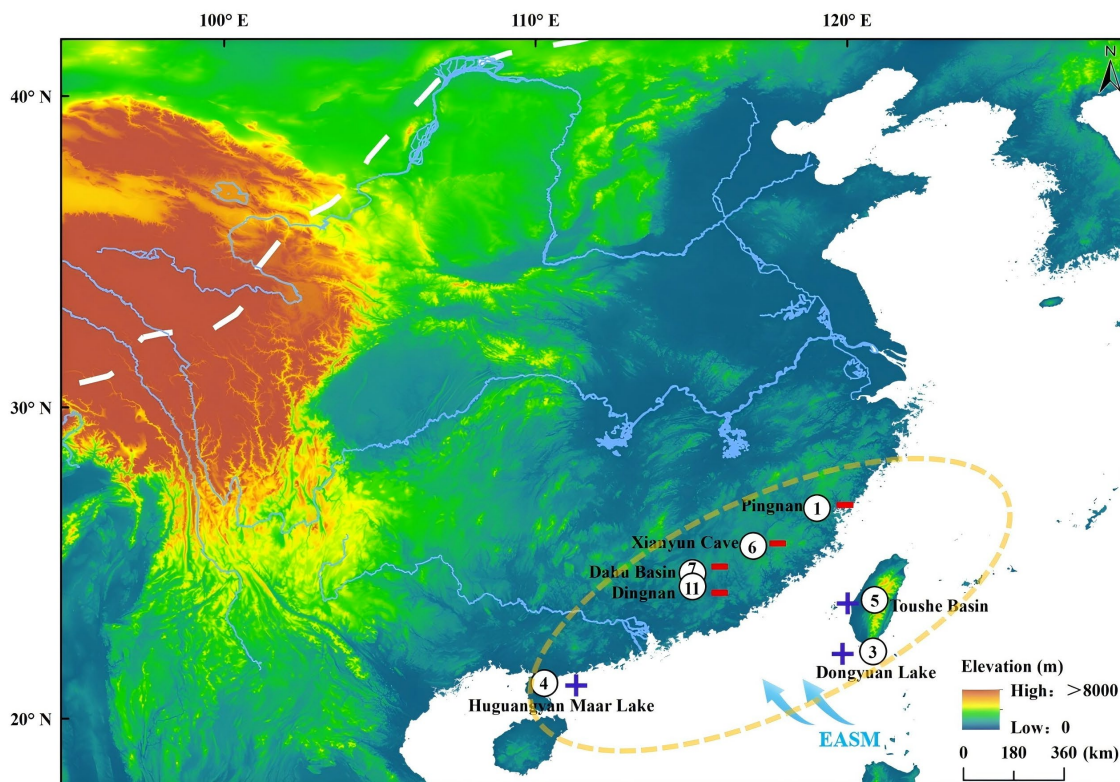
5.1.4. 10,000 yr B.P. (全新世)

全新世以来, 中国东南沿海地区的气候变化存在显著波动。福建屏南孢粉记录的 Z-score 值在全新世早期小于均值, 晚期大于均值, 指示区域气候条件由冷干转为暖湿(图 2(A)) [25]。福建戴云山山地高山孢粉记录的 Z-score 值由全新世早期的大于均值转为全新世晚期小于均值, 指示区域气候条件由暖湿转为冷干(图 2(B)) [26]。广东湖光岩玛珥湖沉积物总有机质(图 2(D)) [29]和孢粉浓度(图 2(E)) [29]的 Z-score 值呈减小趋势, 指示区域转为冷干的气候条件。Toushe 盆地沉积物 $\delta^{13}\text{C}_{\text{TOC}}$ 的 Z-score 值自全新世以来虽存在波动, 但整体小于均值, 指示区域暖湿气候特征(图 2(F)) [31]。

南海冲绳海槽沉积物总有机碳(图 2(I)) [32], 福建福州盆地沉积物磁化率(图 2(L)) [25], 福建龙湖沉积物总有机氮(图 2(P)) [36]、总有机碳(图 2(Q)) [36]的 Z-score 值均呈现自全新世早期小于均值转变为全新世晚期大于均值, 指示区域气候条件由冷干转为暖湿。相反, Retreat 湖沉积物总有机碳(图 2(J)) [30]、C/N 比(图 2(K)) [30]及定南沉积物总有机碳(图 2(M)) [34]记录的 Z-score 值呈现自全新世早期大于均值转

变为全新世晚期小于均值，指示区域气候条件由暖湿转为冷干。中国东南沿海地区沉积物的高有机质含量和高腐殖化程度指示气候寒冷干燥，低有机质含量和低腐殖化程度指示气候温暖湿润[37]。福建天湖山沉积物有机质含量(图 2(N)) [35]、腐殖化程度(图 2(O)) [35]的 Z-score 值呈现全新世早期小于均值转变为全新世晚期大于均值，指示区域气候条件由暖湿转为冷干。福建仙山沉积物腐殖化程度的 Z-score 值自 1950 A.D.以来波动较大，呈逐渐增大趋势，指示区域气候特征转为冷干(图 2(R)) [37]。

综上，全新世以来，中国东南沿海地区的气候变化存在不稳定性，且不同区域之间其气候变化特征具有显著差异(图 2) (图 5)。



注：该图基于自然资源部标准地图服务网站下载的审图号：GS(2016)1590 号的标准地图制作，底图无修改。黄色虚线圆圈代表本研究所界定的中国东南沿海地区的区域范围。蓝色箭头代表东亚夏季风。白色虚线代表中国季风区与非季风区分界线[13]。加号代表区域暖湿的气候特征，减号代表区域冷干的气候特征。

Figure 4. Climatic characteristics of the southeastern coastal region of China during the Last Deglaciation

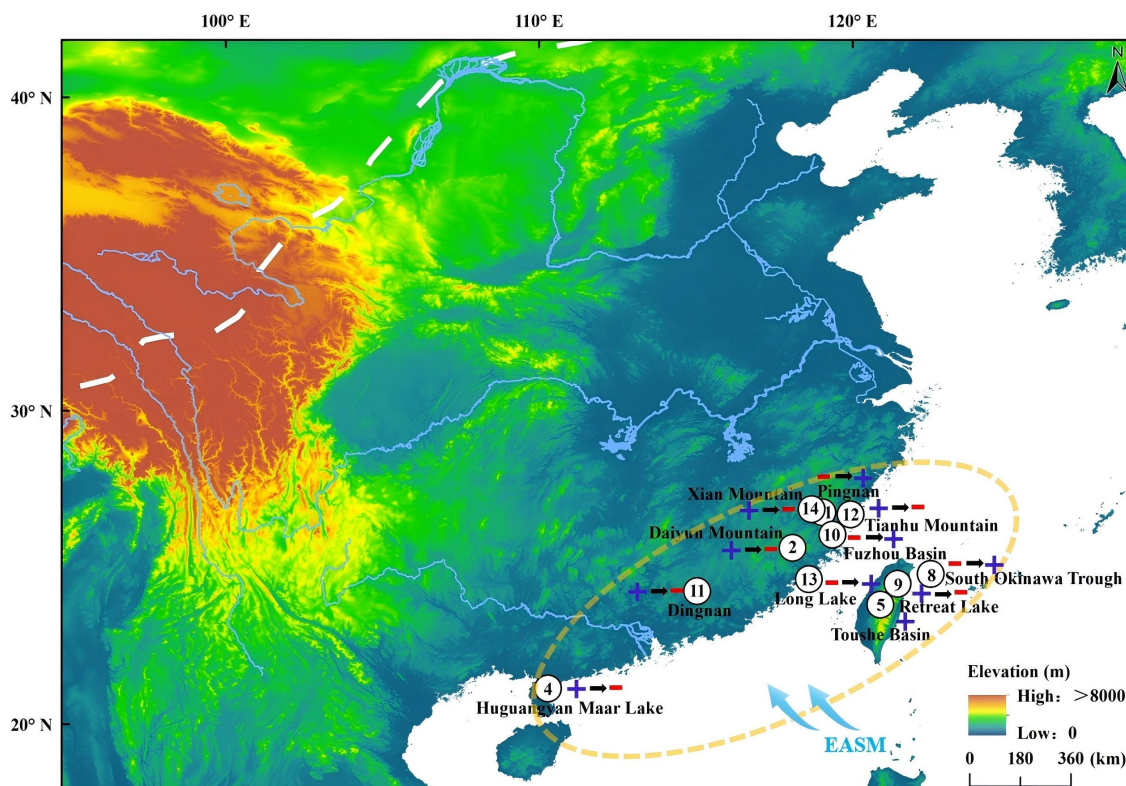
图 4. 末次冰消期中国东南沿海地区的气候特征。

5.2. 全新世以来，中国东南沿海地区气候变化的驱动机制

近年来，随着气候突变事件发生的频率增加，人们开始对未来气候变化越来越关注。全新世是距离人类最近的地质年代。人类社会文明的一切发生、发展、繁荣、进步都出现在此时期。全新世的气候变化与人类社会的发展有密切的关系。所以全新世的千百年尺度的气候波动不仅为评估未来气候变化的发展趋势，以及揭示气候变化和人类生存与发展以及适应具有非常重要的科学价值。

根据植物孢粉、湖泊沉积等多种代用指标记录重建结果发现，中国东南沿海地区全新世存在明显的一系列千百年尺度的气候波动(图 2) (图 5)。目前对中国东南沿海地区全新世千百年尺度的气候波动的原因机制尚不明确，存在各种假设猜想。已经提出了各种驱动力来解释中国东南沿海地区全新世以来的千百年尺度气候异常[9]-[11]。

亚洲夏季风的变化对中国东南沿海地区的水汽输送产生影响,季风的增强使区域内接收的海洋水汽量骤增,大气中的水汽含量增加,导致区域降水量显著增多,形成较为湿润的气候环境;相反,季风的减弱导致海洋水汽输送能力下降,中国东南沿海地区的水汽来源相对减少,大气中的水汽含量降低,降水过程减少且强度减弱,形成较为干燥的气候环境[39][40]。



注:该图基于自然资源部标准地图服务网站下载的审图号:GS(2016)1590号的标准地图制作,底图无修改。蓝色箭头代表东亚夏季风。白色虚线代表中国季风区与非季风区分界线[13]。加号代表区域暖湿的气候特征,减号代表区域冷干的气候特征。黑色箭头代表区域气候条件的转变过程。黄色虚线圆圈代表本研究所界定的中国东南沿海地区的区域范围

Figure 5. Climatic characteristics of the southeastern coastal region of China since the Holocene

图 5. 全新世以来中国东南沿海地区的气候特征

全新世以来,亚洲夏季风呈减弱趋势(图 6(E)),响应于北半球温度和夏季太阳辐射量的下降(图 6),表明在千年尺度上,亚洲夏季风随着太阳辐射的增加而增加,随着太阳辐射的减少而减弱[41]-[44]。因此,因太阳辐射变化所导致的亚洲夏季风变化,对全新世气候产生影响。

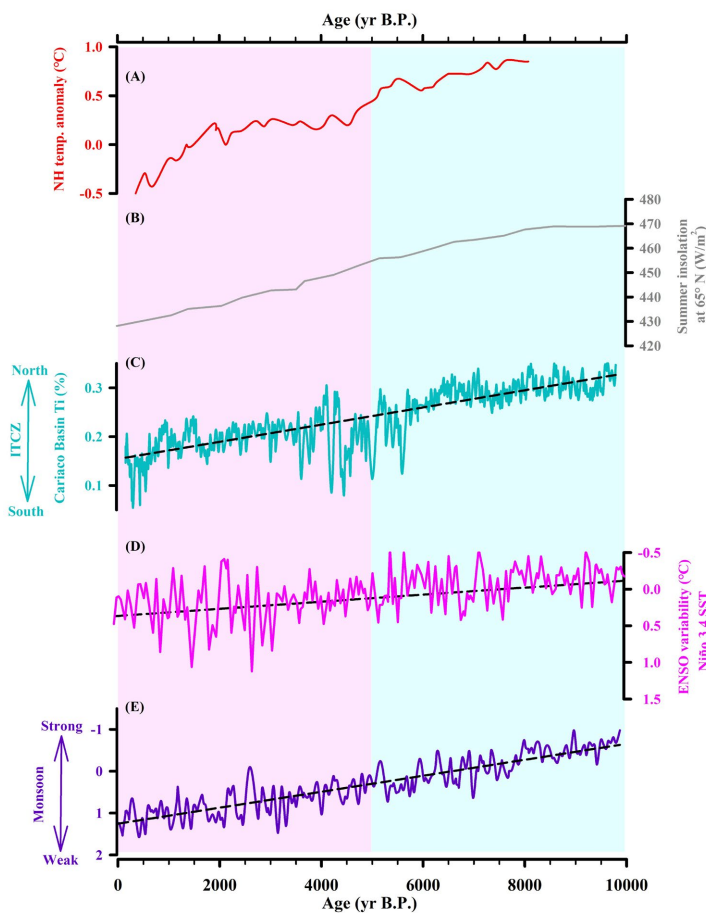
太阳辐射是驱动亚洲夏季风变化的重要外部因素[45],对全新世气候产生影响,而海气环流作用将进一步传输和放大太阳辐射的影响[45]。热带太平洋是巨大的热量储存地,也是大气水汽的重要供应地[43];它的变化不仅影响热带地区气候变化,还通过哈德莱(Hadley)环流等大气环流系统影响中高纬度地区气候[43]。在热带太平洋气候系统中,对中国东南沿海地区影响最大的两个水文系统为赤道辐合带(ITCZ)和厄尔尼诺-南方涛动(ENSO)的变化[46]-[48]。

太阳辐射的变化导致 ITCZ 的南北移动[45]。全新世以来,北半球温度降低(图 6(A)),夏季北半球接收太阳辐射减少(图 6(B)),陆地增温慢,海陆热力性质差异减弱,ITCZ 位置南移(图 6(C)) [49]-[51]。亚洲季风区的降水显著受到哈德莱(Hadley)环流经向水汽输送的影响[52][53]。当 ITCZ 位置北移时,哈德

莱(Hadley)环流上升支对流增强,受海陆热力性质差异的影响,亚洲夏季风也会随之增强或北移[52][53]。当ITCZ位置南移时,哈德莱(Hadley)环流上升支对流减弱,受海陆热力性质差异的影响,亚洲夏季风也会随之减弱或南移(图6)[52][53]。因此,在千年尺度上,ITCZ位置的南北移动响应于太阳辐射,影响亚洲夏季风的强弱(图6),进而对全新世气候变化产生影响。

ENSO活动也对全新世气候变化产生影响[54]-[56]。全新世以来,ENSO活动的强度和频率波动较大(图6(D))[57]-[62]。ENSO活动主要是通过调整海气环流模式来影响亚洲夏季风变化,对全新世气候产生影响。当厄尔尼诺(El Niño)发生时,沃克(Walker)环流减弱,上升支强度减弱,Walker环流向东运移,远离西太平洋暖池[63]-[66]。与此同时,西太平洋副热带高压(The Western Pacific Subtropical High, WPSH)增强,并西伸至中国西南地区[40],上述环流模式的改变导致亚洲夏季风强度减弱(图6);La Niña发生时,情况与之相反[67]-[69]。

综上,全新世以来,中国东南沿海地区气候变化的外部因素是太阳辐射,主导着夏季风周期性变化,进而对气候变化产生影响。热带海气环流传输和放大太阳活动变化的影响,在千年尺度上表现出气候波动事件。在热带太平洋气候系统中,ITCZ的南北移动以及ENSO活动是影响气候变化的重要因素。



(A) 北半球温度异常 (NHTA) [50]; (B) 北纬 65°地区 6~8 月(夏半年)的太阳辐射量[70]; (C) Cariaco 盆地的 Ti 含量 [71], 用以指示热带辐合带(ITCZ)的南北移动; (D) 模拟的厄尔尼诺 - 南方涛动(ENSO)变率[53]; (E) 瞬态模拟中, 夏季(JJA)降水主成分分析的第一主成分(PC1)所代表的亚洲夏季风(ASM)强度[72]。粉色和蓝色条带分别代表 5000~10 yr B.P.和 10,000~5000 yr B.P.两个时段。黑色虚线代表各个记录的趋势线。

Figure 6. Driving mechanisms of climatic changes in the southeastern coastal region of China since the Holocene
图 6. 全新世以来中国东南沿海地区气候变化的驱动机制

6. 结论

本研究通过对末次冰盛期以来中国东南沿海地区的 18 条地质记录进行集成对比分析, 主要得出以下结论:

(1) 末次冰盛期以来, 中国东南沿海地区气候变化存在波动, 经历了多次冷暖、干湿交替阶段, 主要概括为以下 3 个阶段: 25,000~15,000 yr B.P. (末次冰盛期), 中国东南沿海地区以冷干气候条件为主, 在千年尺度上存在振荡; 15,000~10,000 yr B.P. (末次冰消期), 中国东南沿海地区可能存在两种不同的气候模式; 10,000 yr B.P. (全新世以来), 中国东南沿海地区气候变化存在不稳定性, 不同区域之间的气候变化特征具有明显差异。

(2) 全新世以来, 中国东南沿海地区气候变化的主要外部因素是太阳辐射。此外, 热带海气环流会传输和放大太阳活动的影响, 在热带太平洋气候系统中, ITCZ 的南北移动以及 ENSO 活动是影响东南沿海地区气候变化的重要因素。

参考文献

- [1] CLIMAP Project Members (1976) The Surface of the Ice-Age Earth. *Science*, **191**, 1131-1137. <https://doi.org/10.1126/science.191.4232.1131>
- [2] Hughes, P.D., Gibbard, P.L. and Ehlers, J. (2013) Timing of Glaciation during the Last Glacial Cycle: Evaluating the Concept of a Global 'last Glacial Maximum' (LGM). *Earth-Science Reviews*, **125**, 171-198. <https://doi.org/10.1016/j.earscirev.2013.07.003>
- [3] Clark, P.U., Marshall, S.J., Clarke, G.K.C., Hostetler, S.W., Licciardi, J.M. and Teller, J.T. (2001) Freshwater Forcing of Abrupt Climate Change during the Last Glaciation. *Science*, **293**, 283-287. <https://doi.org/10.1126/science.1062517>
- [4] Peltier, W.R. and Fairbanks, R.G. (2006) Global Glacial Ice Volume and Last Glacial Maximum Duration from an Extended Barbados Sea Level Record. *Quaternary Science Reviews*, **25**, 3322-3337. <https://doi.org/10.1016/j.quascirev.2006.04.010>
- [5] Lambeck, K., Rouby, H., Purcell, A., Sun, Y. and Sambridge, M. (2014) Sea Level and Global Ice Volumes from the Last Glacial Maximum to the Holocene. *Proceedings of the National Academy of Sciences of the United States of America*, **111**, 15296-15303. <https://doi.org/10.1073/pnas.1411762111>
- [6] Bowen, D.Q. (2009) Last Glacial Maximum. In: Gornitz, V., Ed., *Encyclopedia of Paleoclimatology and Ancient Environments*, Springer, 1-996.
- [7] Lin, Y., Kopp, R.E., Xiong, H., Hibbert, F.D., Zheng, Z., Yu, F., et al. (2025) Modern Sea-Level Rise Breaks 4,000-Year Stability in Southeastern China. *Nature*, **646**, 856-864. <https://doi.org/10.1038/s41586-025-09600-z>
- [8] Li, F., Zhou, J., Ren, J., Chen, F., Zhou, X., Olsen, J.W., et al. (2023) Environmental Reconstruction and Dating of Shixiakou Locality 1 on China's West Loess Plateau: Implications for Human Adaptive Changes Apparent during the Last Glacial Maximum (LGM) and Post-LGM Periods. *Archaeological and Anthropological Sciences*, **16**, Article No. 15. <https://doi.org/10.1007/s12520-023-01922-1>
- [9] Dong, G., Zhou, W., Fu, Y., Xian, F. and Zhang, L. (2024) The LGM Termination in the Southeastern Tibetan Plateau: View from High-Frequency LGM Glacier Fluctuations in the Boshula Mountain Range. *Quaternary Science Reviews*, **344**, Article ID: 108971. <https://doi.org/10.1016/j.quascirev.2024.108971>
- [10] Lu, H., Wu, H. and Meadows, M. (2024) Asian Monsoon Variations over the Past 21 Ka: An Introduction. *Global and Planetary Change*, **237**, Article ID: 104452. <https://doi.org/10.1016/j.gloplacha.2024.104452>
- [11] Wang, B., Wu, R. and Lau, K. (2001) Interannual Variability of the Asian Summer Monsoon: Contrasts between the Indian and the Western North Pacific-East Asian Monsoons. *Journal of Climate*, **14**, 4073-4090. [https://doi.org/10.1175/1520-0442\(2001\)014<4073:ivotas>2.0.co;2](https://doi.org/10.1175/1520-0442(2001)014<4073:ivotas>2.0.co;2)
- [12] Wang, B. and Ho, L. (2002) Rainy Season of the Asian-Pacific Summer Monsoon. *Journal of Climate*, **15**, 386-398. [https://doi.org/10.1175/1520-0442\(2002\)015<0386:rsotap>2.0.co;2](https://doi.org/10.1175/1520-0442(2002)015<0386:rsotap>2.0.co;2)
- [13] Xu, D., Lu, H., Chu, G., Shen, C., Li, F., Wu, J., et al. (2020) Asynchronous 500-Year Summer Monsoon Rainfall Cycles between Northeast and Central China during the Holocene. *Global and Planetary Change*, **195**, Article ID: 103324. <https://doi.org/10.1016/j.gloplacha.2020.103324>
- [14] Lu, R., Jia, F., Gao, S., Shang, Y., Li, J. and Zhao, C. (2015) Holocene Aeolian Activity and Climatic Change in Qinghai Lake Basin, Northeastern Qinghai-Tibetan Plateau. *Palaeogeography, Palaeoclimatology, Palaeoecology*, **430**, 1-10.

- <https://doi.org/10.1016/j.palaeo.2015.03.044>
- [15] Selvaraj, K., Chen, C.T.A. and Lou, J. (2007) Holocene East Asian Monsoon Variability: Links to Solar and Tropical Pacific Forcing. *Geophysical Research Letters*, **34**, L01703. <https://doi.org/10.1029/2006gl028155>
- [16] Zhong, W., Cao, J., Xue, J., Ouyang, J., Tang, X., Yin, H., *et al.* (2014) Late Holocene Monsoon Climate as Evidenced by Proxy Records from a Lacustrine Sediment Sequence in Western Guangdong, South China. *Journal of Asian Earth Sciences*, **80**, 56-62. <https://doi.org/10.1016/j.jseae.2013.10.030>
- [17] Xu, L., Liu, Y., Sun, Q., Chen, J., Cheng, P. and Chen, Z. (2017) Climate Change and Human Occupations in the Lake Daihai Basin, North-Central China over the Last 4500 Years: A Geo-Archeological Perspective. *Journal of Asian Earth Sciences*, **138**, 367-377. <https://doi.org/10.1016/j.jseae.2017.02.019>
- [18] Liu, F., Zhang, Y., Feng, Z., Hou, G., Zhou, Q. and Zhang, H. (2010) The Impacts of Climate Change on the Neolithic Cultures of Gansu-Qinghai Region during the Late Holocene Megathermal. *Journal of Geographical Sciences*, **20**, 417-430. <https://doi.org/10.1007/s11442-010-0417-1>
- [19] Hu, C., Henderson, G.M., Huang, J., Xie, S., Sun, Y. and Johnson, K.R. (2008) Quantification of Holocene Asian Monsoon Rainfall from Spatially Separated Cave Records. *Earth and Planetary Science Letters*, **266**, 221-232. <https://doi.org/10.1016/j.epsl.2007.10.015>
- [20] Tan, L., Cai, Y., Cheng, H., Edwards, L.R., Gao, Y., Xu, H., *et al.* (2018) Centennial- to Decadal-Scale Monsoon Precipitation Variations in the Upper Hanjiang River Region, China over the Past 6650 Years. *Earth and Planetary Science Letters*, **482**, 580-590. <https://doi.org/10.1016/j.epsl.2017.11.044>
- [21] Herzschuh, U., Winter, K., Wünnemann, B. and Li, S. (2006) A General Cooling Trend on the Central Tibetan Plateau Throughout the Holocene Recorded by the Lake Zigetang Pollen Spectra. *Quaternary International*, **154**, 113-121. <https://doi.org/10.1016/j.quaint.2006.02.005>
- [22] Wen, R., Xiao, J., Chang, Z., Zhai, D., Xu, Q., Li, Y., *et al.* (2010) Holocene Climate Changes in the Mid-High-Latitude-Monsoon Margin Reflected by the Pollen Record from Hulun Lake, Northeastern Inner Mongolia. *Quaternary Research*, **73**, 293-303. <https://doi.org/10.1016/j.yqres.2009.10.006>
- [23] Cleveland, W.S. (1979) Robust Locally Weighted Regression and Smoothing Scatterplots. *Journal of the American Statistical Association*, **74**, 829-836. <https://doi.org/10.1080/01621459.1979.10481038>
- [24] Wilks, D.S. (2011) *Statistical Methods in the Atmospheric Sciences*. 3rd Edition, Academic Press.
- [25] Yue, Y., Zheng, Z., Huang, K., Chevalier, M., Chase, B.M., Carré, M., *et al.* (2012) A Continuous Record of Vegetation and Climate Change over the Past 50,000years in the Fujian Province of Eastern Subtropical China. *Palaeogeography, Palaeoclimatology, Palaeoecology*, **365**, 115-123. <https://doi.org/10.1016/j.palaeo.2012.09.018>
- [26] Zhao, L., Ma, C., Leipe, C., Long, T., Liu, K., Lu, H., *et al.* (2017) Holocene Vegetation Dynamics in Response to Climate Change and Human Activities Derived from Pollen and Charcoal Records from Southeastern China. *Palaeogeography, Palaeoclimatology, Palaeoecology*, **485**, 644-660. <https://doi.org/10.1016/j.palaeo.2017.06.035>
- [27] Chen, L., Zhou, W., Zhang, Y., Zheng, Y. and Huang, X. (2020) Postglacial Floral and Climate Changes in Southeastern China Recorded by Distributions of N-Alkan-2-Ones in the Dahu Sediment-Peat Sequence. *Palaeogeography, Palaeoclimatology, Palaeoecology*, **538**, Article ID: 109448. <https://doi.org/10.1016/j.palaeo.2019.109448>
- [28] <https://doi.org/10.1016/j.palaeo.2016.02.048>
- [29] Wang, X., Chu, G., Sheng, M., Zhang, S., Li, J., Chen, Y., *et al.* (2016) Millennial-Scale Asian Summer Monsoon Variations in South China since the Last Deglaciation. *Earth and Planetary Science Letters*, **451**, 22-30. <https://doi.org/10.1016/j.epsl.2016.07.006>
- [30] <https://doi.org/10.1016/j.quaint.2010.01.015>
- [31] <https://doi.org/10.1016/j.jseae.2012.12.005>
- [32] <https://doi.org/10.1016/j.palaeo.2018.11.026>
- [33] Zhou, W., Xie, S., Meyers, P.A. and Zheng, Y. (2005) Reconstruction of Late Glacial and Holocene Climate Evolution in Southern China from Geolipids and Pollen in the Dingnan Peat Sequence. *Organic Geochemistry*, **36**, 1272-1284. <https://doi.org/10.1016/j.orggeochem.2005.04.005>
- [34] Zhang, H., Li, Z.Z., Jiang, X.Y., Jin, J.H., Hu, F.G., Zhao, Q., *et al.* (2012) Paleo-Climatic Significance for Nearly 10 ka Revealed by Tianhushan Peat Record in the Northern Fujian. *Journal of Ningxia University (Nature Science Edition)*, **33**, 120-124.
- [35] Wang, W.G. and Ye, X. (2009) Environmental Significance of Longhu Lake Sediments in the Middle and Late Holocene, Jin-jiang, Fujian. *Journal of Palaeogeography-English*, **11**, 348-354.
- [36] Hu, F.G., Li, Z.Z., Jin, J.H., Zhang, H. and Zhao, Q. (2012) The Past 1, 500 Years Climate Change Recorded in the Peat Humification at Xianshan in Northern of Fujian Province. *Carpathian Journal of Earth and Environmental Sciences*, **3**,

712-720.

- [37] Cheng, X., Xue, G., Chen, Q.M., Wu, Y., Ma, L., Wang, G.Z., *et al.* (2026) Hydroclimate Changes during the Last Deglaciation in Central China Inferred from Speleothem Multiple Proxies. *Global and Planetary Change*, **256**, Article ID: 105187. <https://doi.org/10.1016/j.gloplacha.2025.105187>
- [38] Cui, M.Y., Hong, H., Sun, X.S., Jiang, X.Y. and Cai, B.G. (2018) The Gradual Change Characteristics at the End of the Younger Dryas Event Inferred from a Speleothem Record from Xianyun Cave, Fujian Province. *Quaternary Science*, **38**, 711-719.
- [39] Tan, M. (2013) Circulation Effect: Response of Precipitation $\delta^{18}\text{O}$ to the ENSO Cycle in Monsoon Regions of China. *Climate Dynamics*, **42**, 1067-1077. <https://doi.org/10.1007/s00382-013-1732-x>
- [40] Tan, L., Shen, C., Löwemark, L., Chawchai, S., Edwards, R.L., Cai, Y., *et al.* (2019) Rainfall Variations in Central Indo-Pacific over the Past 2,700 Y. *Proceedings of the National Academy of Sciences of the United States of America*, **116**, 17201-17206. <https://doi.org/10.1073/pnas.1903167116>
- [41] Solanki, S.K., Usoskin, I.G., Kromer, B., Schüssler, M. and Beer, J. (2004) Unusual Activity of the Sun during Recent Decades Compared to the Previous 11,000 Years. *Nature*, **431**, 1084-1087. <https://doi.org/10.1038/nature02995>
- [42] Wan, N., Li, H., Liu, Z., Yang, H., Yuan, D. and Chen, Y. (2011) Spatial Variations of Monsoonal Rain in Eastern China: Instrumental, Historic and Speleothem Records. *Journal of Asian Earth Sciences*, **40**, 1139-1150. <https://doi.org/10.1016/j.jseaes.2010.10.003>
- [43] Cheng, H., Edwards, R.L., Sinha, A., Spötl, C., Yi, L., Chen, S., *et al.* (2016) The Asian Monsoon over the Past 640,000 Years and Ice Age Terminations. *Nature*, **534**, 640-646. <https://doi.org/10.1038/nature18591>
- [44] Mohtadi, M., Prange, M. and Steinke, S. (2016) Palaeoclimatic Insights into Forcing and Response of Monsoon Rainfall. *Nature*, **533**, 191-199. <https://doi.org/10.1038/nature17450>
- [45] Zhang, P., Cheng, H., Edwards, R.L., Chen, F., Wang, Y., Yang, X., *et al.* (2008) A Test of Climate, Sun, and Culture Relationships from an 1810-Year Chinese Cave Record. *Science*, **322**, 940-942. <https://doi.org/10.1126/science.1163965>
- [46] Waliser, D.E. and Gautier, C. (1993) A Satellite-Derived Climatology of the ITCZ. *Journal of Climate*, **6**, 2162-2174. [https://doi.org/10.1175/1520-0442\(1993\)006<2162:asdcot>2.0.co;2](https://doi.org/10.1175/1520-0442(1993)006<2162:asdcot>2.0.co;2)
- [47] Dong, B.W. and Sutton, R.T. (2002) Adjustment of the Coupled Ocean-Atmosphere System to a Sudden Change in the Thermohaline Circulation. *Geophysical Research Letters*, **29**, 18-1-18-4. <https://doi.org/10.1029/2002gl015229>
- [48] Griffiths, M.L., Kimbrough, A.K., Gagan, M.K., Drysdale, R.N., Cole, J.E., Johnson, K.R., *et al.* (2016) Western Pacific Hydroclimate Linked to Global Climate Variability over the Past Two Millennia. *Nature Communications*, **7**, Article No. 11719. <https://doi.org/10.1038/ncomms11719>
- [49] Moy, C.M., Seltzer, G.O., Rodbell, D.T. and Anderson, D.M. (2002) Variability of El Niño/southern Oscillation Activity at Millennial Timescales during the Holocene Epoch. *Nature*, **420**, 162-165. <https://doi.org/10.1038/nature01194>
- [50] Marcott, S.A., Shakun, J.D., Clark, P.U. and Mix, A.C. (2013) A Reconstruction of Regional and Global Temperature for the Past 11,300 Years. *Science*, **339**, 1198-1201. <https://doi.org/10.1126/science.1228026>
- [51] Wang, P.X., Wang, B., Cheng, H., Fasullo, J., Guo, Z., Kiefer, T., *et al.* (2017) The Global Monsoon across Time Scales: Mechanisms and Outstanding Issues. *Earth-Science Reviews*, **174**, 84-121. <https://doi.org/10.1016/j.earscirev.2017.07.006>
- [52] Schneider, T., Bischoff, T. and Haug, G.H. (2014) Migrations and Dynamics of the Intertropical Convergence Zone. *Nature*, **513**, 45-53. <https://doi.org/10.1038/nature13636>
- [53] Zhao, K., Wang, Y., Edwards, R.L., Cheng, H., Liu, D., Kong, X., *et al.* (2016) Contribution of ENSO Variability to the East Asian Summer Monsoon in the Late Holocene. *Palaeogeography, Palaeoclimatology, Palaeoecology*, **449**, 510-519. <https://doi.org/10.1016/j.palaeo.2016.02.044>
- [54] Kumar, K.K., Rajagopalan, B., Hoerling, M., Bates, G. and Cane, M. (2006) Unraveling the Mystery of Indian Monsoon Failure during El Niño. *Science*, **314**, 115-119. <https://doi.org/10.1126/science.1131152>
- [55] Yan, H., Sun, L., Wang, Y., Huang, W., Qiu, S. and Yang, C. (2011) A Record of the Southern Oscillation Index for the Past 2,000 Years from Precipitation Proxies. *Nature Geoscience*, **4**, 611-614. <https://doi.org/10.1038/ngeo1231>
- [56] Berkelhammer, M., Sinha, A., Mudelsee, M., Cheng, H., Yoshimura, K. and Biswas, J. (2014) On the Low-Frequency Component of the Enso-Indian Monsoon Relationship: A Paired Proxy Perspective. *Climate of the Past*, **10**, 733-744. <https://doi.org/10.5194/cp-10-733-2014>
- [57] Rein, B., Lückge, A., Reinhardt, L., Sirocko, F., Wolf, A. and Dullo, W. (2005) El Niño Variability off Peru during the Last 20,000 Years. *Paleoceanography*, **20**, PA4003. <https://doi.org/10.1029/2004pa001099>
- [58] Conroy, J.L., Overpeck, J.T., Cole, J.E., Shanahan, T.M. and Steinitz-Kannan, M. (2008) Holocene Changes in Eastern Tropical Pacific Climate Inferred from a Galápagos Lake Sediment Record. *Quaternary Science Reviews*, **27**, 1166-1180.

- <https://doi.org/10.1016/j.quascirev.2008.02.015>
- [59] Toth, L.T., Aronson, R.B., Vollmer, S.V., Hobbs, J.W., Urrego, D.H., Cheng, H., *et al.* (2012) ENSO Drove 2500-Year Collapse of Eastern Pacific Coral Reefs. *Science*, **337**, 81-84. <https://doi.org/10.1126/science.1221168>
- [60] Zhang, Z., Leduc, G. and Sachs, J.P. (2014) El Niño Evolution during the Holocene Revealed by a Biomarker Rain Gauge in the Galápagos Islands. *Earth and Planetary Science Letters*, **404**, 420-434. <https://doi.org/10.1016/j.epsl.2014.07.013>
- [61] Wu, J., Liu, Q., Cui, Q.Y., Xu, D.K., Wang, L., Shen, C.M., *et al.* (2019) Shrinkage of East Asia Winter Monsoon Associated with Increased ENSO Events since the Mid-Holocene. *Journal of Geophysical Research: Atmospheres*, **124**, 3839-3848. <https://doi.org/10.1029/2018jd030148>
- [62] Du, X., Hendy, I., Hinnov, L., Brown, E., Zhu, J. and Poulsen, C.J. (2021) High-Resolution Interannual Precipitation Reconstruction of Southern California: Implications for Holocene ENSO Evolution. *Earth and Planetary Science Letters*, **554**, Article ID: 116670. <https://doi.org/10.1016/j.epsl.2020.116670>
- [63] Rasmusson, E.M. and Carpenter, T.H. (1983) The Relationship between Eastern Equatorial Pacific Sea Surface Temperatures and Rainfall over India and Sri Lanka. *Monthly Weather Review*, **111**, 517-528. [https://doi.org/10.1175/1520-0493\(1983\)111<0517:trbeep>2.0.co;2](https://doi.org/10.1175/1520-0493(1983)111<0517:trbeep>2.0.co;2)
- [64] Ropelewski, C.F. and Halpert, M.S. (1996) Quantifying Southern Oscillation-Precipitation Relationships. *Journal of Climate*, **9**, 1043-1059. [https://doi.org/10.1175/1520-0442\(1996\)009<1043:qsopr>2.0.co;2](https://doi.org/10.1175/1520-0442(1996)009<1043:qsopr>2.0.co;2)
- [65] Zhang, J., Liang, M., Li, T., Chen, C. and Li, J. (2022) Asian-Australian Monsoon Evolution over the Last Millennium Linked to ENSO in Composite Stalagmite $\delta^{18}\text{O}$ and $\delta^{13}\text{C}$ Records. *Quaternary Science Reviews*, **281**, Article ID: 107420. <https://doi.org/10.1016/j.quascirev.2022.107420>
- [66] Duan, R., Li, T., Li, J., Spötl, C., Li, H., Wang, H., *et al.* (2023) Karst-Ecological Changes during the Middle and Late Holocene in Southwest China Revealed by $\delta^{18}\text{O}$ and $\delta^{13}\text{C}$ Records in a Stalagmite. *Palaeogeography, Palaeoclimatology, Palaeoecology*, **615**, Article ID: 111437. <https://doi.org/10.1016/j.palaeo.2023.111437>
- [67] Chen, C. and Li, T. (2018) Geochemical Characteristics of Cave Drip Water Respond to ENSO Based on a 6-Year Monitoring Work in Yangkou Cave, Southwest China. *Journal of Hydrology*, **561**, 896-907. <https://doi.org/10.1016/j.jhydrol.2018.04.061>
- [68] Zhang, J. and Li, T. (2019) Seasonal and Interannual Variations of Hydrochemical Characteristics and Stable Isotopic Compositions of Drip Waters in Furong Cave, Southwest China Based on 12 Years' Monitoring. *Journal of Hydrology*, **572**, 40-50. <https://doi.org/10.1016/j.jhydrol.2019.02.052>
- [69] Dearing, J.A., Jones, R.T., Shen, J., Yang, X., Boyle, J.F., Foster, G.C., *et al.* (2007) Using Multiple Archives to Understand Past and Present Climate-Human-Environment Interactions: The Lake Erhai Catchment, Yunnan Province, China. *Journal of Paleolimnology*, **40**, 3-31. <https://doi.org/10.1007/s10933-007-9182-2>
- [70] Laskar, J., Robutel, P., Joutel, F., Gastineau, M., Correia, A.C.M. and Levrard, B. (2004) A Long-Term Numerical Solution for the Insolation Quantities of the Earth. *Astronomy & Astrophysics*, **428**, 261-285. <https://doi.org/10.1051/0004-6361:20041335>
- [71] Haug, G.H., Hughen, K.A., Sigman, D.M., Peterson, L.C. and Röhl, U. (2001) Southward Migration of the Intertropical Convergence Zone through the Holocene. *Science*, **293**, 1304-1308. <https://doi.org/10.1126/science.1059725>
- [72] Jin, L., Schneider, B., Park, W., Latif, M., Khon, V. and Zhang, X. (2014) The Spatial-Temporal Patterns of Asian Summer Monsoon Precipitation in Response to Holocene Insolation Change: A Model-Data Synthesis. *Quaternary Science Reviews*, **85**, 47-62. <https://doi.org/10.1016/j.quascirev.2013.11.004>